Computational and Structural Biotechnology Journal 21 (2023) 3680–3689

Contents lists available at ScienceDirect

Computational and Structural Biotechnology Journal

journal homepage: www.elsevier.com/locate/csbj

Research article

Integrated approaches for the recognition of small molecule inhibitors for Toll-like receptor 4

Shailya Verma [a], Purushotham Reddy [a,b], R. Sowdhamini [a,c,d,*]

[a] National Centre for Biological Sciences (TIFR), GKVK campus, Bangalore 560065, India
[b] NMR-Analytical research and development, Aurobindo Pharma, Research center-II, Hyderabad, Telangana 502307, India
[c] Molecular Biophysics Unit, Indian Institute of Science, Bangalore 560012, India
[d] Institute of Bioinformatics and Applied Biotechnology, Electronic City, 560100, India

ARTICLE INFO

Keywords:
Toll-like receptor
TIR domain
Autoimmune
Virtual screening
MD simulations
Reporter assay
NMR

ABSTRACT

Toll-like receptors (TLRs) are pattern recognition receptors present on the surface of cells playing a crucial role in innate immunity. One of the TLRs, TLR4, recognizes LPS (Lipopolysaccharide) as its ligand leading to the release of anti-inflammatory mediators as well as pro-inflammatory cytokines through signal transduction and domain recruitment. TLR4 homodimerizes at its intracellular TIR (Toll/interleukin-1 receptor) domain that helps in the recruitment of the TRAM/TICAM2 (TIR domain-containing adaptor molecule 2) molecule. TRAM also contains TIR domain which in turn, dimerizes and functions as an adapter protein to further recruit TRIF/TICAM1 (TIR domain-containing adaptor molecule 1) protein for mediating downstream signaling. Apart from LPS, TLR4 also recognizes endogenous ligands like fibrinogen, HMGB1, and hyaluronan in autoimmune conditions and sepsis. We employed computational approaches to target TRAM and recognize small molecule inhibitors from small molecules of natural origin, as contained in the Super Natural II database. Finally, cell reporter assays and NMR studies enabled the identification of promising lead compounds. Hence, this study aims to attenuate the signaling of the TLR4-TRAM-TRIF cascade in these auto-inflammatory conditions.

1. Introduction

Toll-like receptors (TLR) play a crucial role in the innate immune response by recognizing PAMPs (Pathogen Associated Molecular Patterns) and DAMPs (Danger Associated Molecular Patterns) as their ligands. The exogenous PAMP are derived from bacterial or viral sources, whereas the DAMP includes endogenous proteins [1]. There are 10 known TLRs in humans and each of them identifies a different ligand.

Some of these TLRs are present on the plasma membrane (1, 2, 4, 5, 6, 10), whereas others (3, 4, 7, 8, 9) are located on the endosomes. Unlike others, TLR4 is present on the plasma membrane as well as the endosome. Structurally, TLRs are type I transmembrane receptors with an extracellular domain that has Leucine Rich Repeat (LRR), followed by a transmembrane region and an intracellular TIR domain (Toll/interleukin-1 receptor) [2]. The cytoplasmic TIR domain is approximately 200 amino acids. It promotes the assembly of signaling complexes via protein-protein interactions. The primordial function of TIR domain containing proteins a per the InterPro Toll/interleukin-1 receptor homology (TIR) domain entry (IPR000157) is of a self-association-dependent nicotinamide dinucleotide (NAD(+)) cleaving enzyme (NADase) activity that cleaves NAD(+) into nicotinamide (Nam) and ADP-ribose (ADPR), cyclic ADPR (cADPR) or variant cADPR (v-cADPR), with catalytic cleavage executed by a conserved Glutamic acid [3–5].

On identification of the ligands, the TLR forms homo or hetero dimers and recruits the adaptor molecules like MyD88, TIRAP, TRIF (also called TICAM1 and is specific to TLR4 and TLR3), TRAM (also called TICAM2 and is exclusive for TLR4 signaling pathway). The MyD88 & TIRAP dependent pathway ultimately releases pro-inflammatory cytokines, NF-κB, Tumor Necrosis Factor alpha (TNF-α), interleukin (IL-)1β, IL-6, and chemokines like Monocyte Chemoattractant Protein 1 (MCP-1), Macrophage Inflammatory Protein 3α (MIP-3α), and IL-8. Whereas TRIF & TRAM pathway releases both pro-inflammatory cytokines as well as anti-inflammatory mediators like Interferon Regulatory Factor 3 (IRF3), beta interferon (IFN-β), delayed NF-κB activation, type 1 IFN-α/β, IFN-α-inducible protein 10 (IP-10), MCP-5, RANTES, and nitric oxide release [1,6]. A schematic representing the TLR signaling pathway with adaptors and mediators is shown in Fig. 1.

* Corresponding author at: National Centre for Biological Sciences (TIFR), GKVK campus, Bangalore, 560065, India.
E-mail address: mini@ncbs.res.in (R. Sowdhamini).

https://doi.org/10.1016/j.csbj.2023.07.026
Received 21 March 2023; Received in revised form 8 July 2023; Accepted 19 July 2023
Available online 22 July 2023

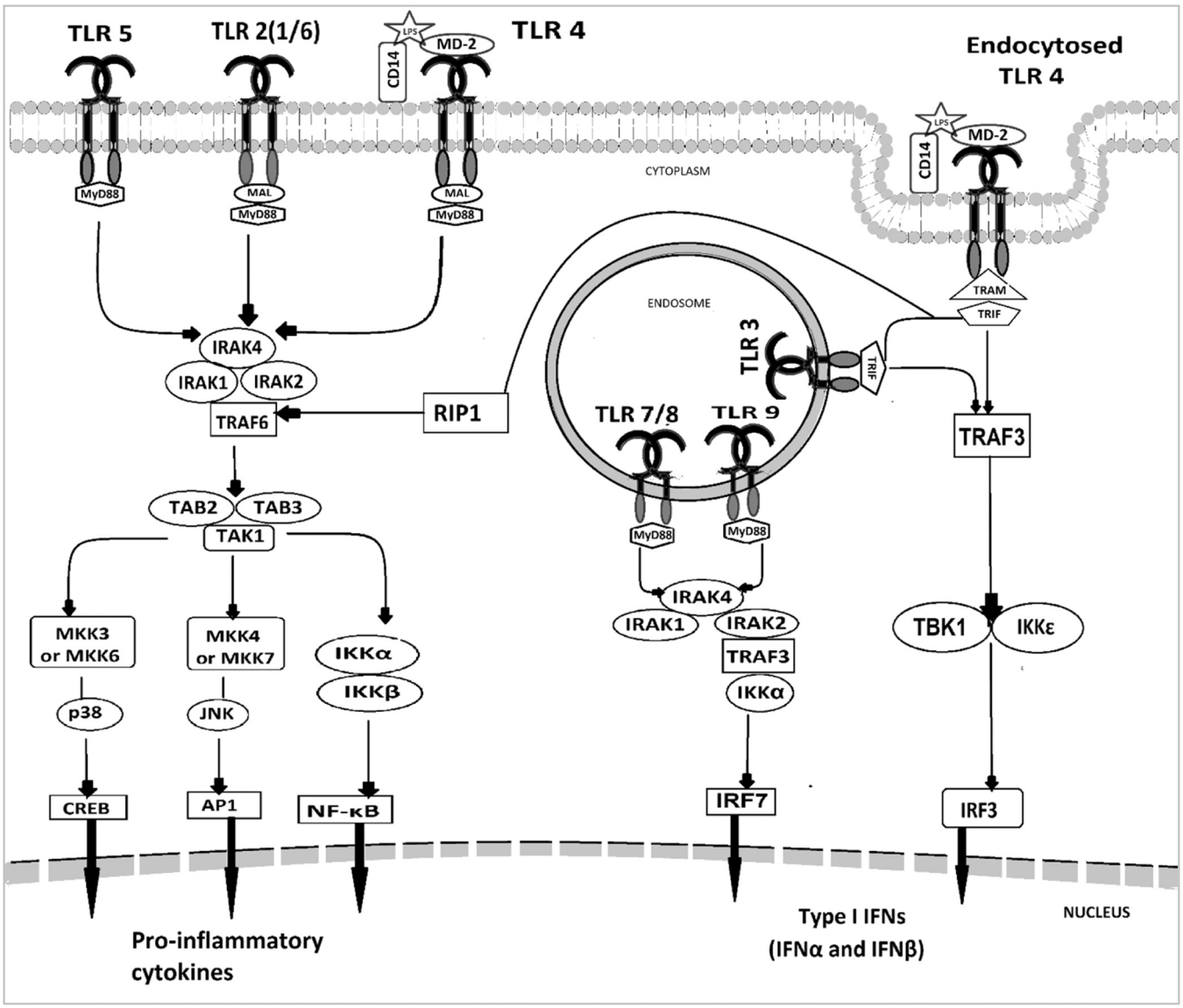

Fig. 1. Schematic of Toll-like receptor downstream signaling pathway.

TLR4 exhibits both MyD88-dependent as well as TRAM dependent pathway. This TLR recognizes Lipopolysaccharides (LPS) as ligands and upon binding to hexa-acylated LPS, CD-14 transfers it to MD-2 causing the dimerization and then recruits the adaptor molecules to control the downstream processes [7]. This study aims to target TLR4-TRAM signaling. Upon recognition of ligand, TLR4 forms a homodimer of the TIR domain with the help of its BB-loop interaction and associates in a twofold symmetry [8]. These BB-loops form the interface which helps in the recruitment of the TRAM adaptor molecule, which also forms dimers symmetrically in a twofold axis along its BB-loop. The TRAM dimer recruits the TRIF through interaction between its EDD & TS site and RK & QI site of TRIF. These crucial residues have been found through mutational studies [9]. These residues are very important for interactions, so they were used in selecting the docking site.

The role of TLR4 is seen evident in sepsis, inflammatory conditions as well as cancer. Also, if the LPS is not controlled properly it can lead to septic shock syndrome which is a major cause of death in patients in the ICU [10]. Besides, these there are several literature reports that support the instances, where sepsis occurs as the worst outcome of host-pathogen interactions, that is a leading cause of death [10,11]. Sepsis is developed equally by the gram-positive and gram-negative bacteria where exaggerated immune trigger leads to multi-organ failure and septic shock. These gram-negative bacteria contain the LPS that contributes to sepsis development, also the septic shock is due to the amplified body immune response rather than the infection [12]. Additionally, there has been various TLR inhibitors clinically evaluated to manage the sepsis conditions [13]. However, all the currently investigated inhibitors are targeting at the level of TLRs. Our objective through this study is to target such overamplified signaling in case of TLR4, with the help of the TRAM adaptor protein.

The aim is to search for small molecule therapeutic that attenuates or enhances TLR4-mediated signaling. The approach we have taken here is to search for a novel compound that targets TRAM and hinders its role as an adaptor.

A previous study from the lab had used TRAM as a target [14] since A46-VIPER motif from vaccinia virus producing protein is known to disrupt TRAM-TLR interactions. The VIPER peptide representing the VIPER motif is now used in the field as TLR4 inhibitor [15]. It binds to the TIR domain of the adaptor proteins thereby masking the binding sites on TRAM and MAL and inhibiting the downstream signaling. Also, another study suggests these VIPER motif being particularly important for TRAM antagonism, as seen in case of Mal-deficient immortalized mouse bone marrow-derived macrophage (iBMDMs) [16]. These peptide do not interacts with MAL (MyD88 mediated pathway) in vitro [17].

Although the exact binding site is not fully elucidated, in our previous attempt we used homology modeling and molecular docking approach to identify potential binding sites on TRAM (focusing on BB-loop and C^{α} helix). In the previous study ligands were screened from the ZINC database and top 12 compounds were selected as potential hits [14]. In this study, we present the findings of virtual screening using small molecules of natural origin from Supernatural Database [18]. We have also validated the small molecules using cell-based assay and NMR titrations and report two promising candidate small molecules which bind better than VIPER motif.

2. Materials and methods

2.1. Virtual screening pipeline

A virtual screening pipeline was followed using Glide [19] from Schrodinger Suite. The protein coordinates were retrieved from PDB (PDB ID: 2M1W, H117C) and the ligand library was prepared from the Supernatural II database which contains all compounds of natural origin (3,25,287 small molecules) [18]. All small molecules and proteins were prepared and optimized at pH = 7.4 using Ligprep and the Protein preparation module of Glide. Ligprep also considers the tautomers and all possible conformations while preparing the ligand library, thereby 4, 31,685 ligands were generated. Further Site Map was used to predict the potential binding site on the protein [20]. Docking was performed through a series of hierarchical filters i.e. HTVS mode (high-throughput virtual screening) for efficiently enriching million compound libraries, to the SP mode (standard precision) for reliably docking tens to hundreds of thousands of ligands with high accuracy, to the XP mode (extra precision) where further elimination of false positives is accomplished by more extensive sampling and advanced scoring, resulting in even higher enrichment. Each step proceeded with the top 10 % from the previous one. The HTVS filtered the library to around 3,40,000, SP filtered to around 34,000 and, XP filtered to around 3000 small molecules respectively. Latter QikProp descriptors were used to select compounds with 95 % drug-like properties using ADME criteria (absorption, distribution, metabolism, and excretion) [21]. Binding energy was calculated using MM-GBSA (molecular mechanics energies combined with generalized Born and surface area continuum solvation) from the Prime module [22]. The formula for ΔG calculation by MMGBSA is as follows: ΔG (bind) = E_complex (minimized) - (E_ligand (minimized) + E_receptor (minimized). After this step top 3000 compounds, in each case, were clustered using CANVAS hierarchical fingerprinting and Schrodinger's interaction-based fingerprint [23,24]. MOLPRINT2D fingerprint method was used and clustering was tried using all available options (Average, Ward, Single, Centroid, Mc Quitty, Complete, Weighted Centroid, Flexible β and Schrodinger). Average and Flexible β methods were chosen as these two methods gave the best clusters. List of clusters centroids from these methods along with top 10 MMGBSA ΔG (bind) score compounds were combined and the top score compounds were then sorted and list of purchasable ones were made.

2.2. Molecular dynamics simulations

Further Molecular Dynamics Simulations were performed using Desmond for protein-ligand complex initially for 20 ns. We performed an initial all-atom Molecular Dynamics Simulations (MD) using Desmond (Schrodinger suite) [25]. The Protein-ligand complex with the best scores was selected after XP docking. The system builder was used with the TIP4P solvent model and default boundary conditions [26]. Using the OPLS3e force field and adding ions for neutralization the set-up file was prepared. This was further taken forward for simulation of 20 ns at a temperature of 300 K and Pressure of 1.013 bar. Further, the whole system was relaxed through energy minimization before simulation and detailed interaction analysis was performed. For ligands that showed good results in reporter assay, the MD simulations were extended to 100 ns.

2.3. Small molecule ligands for experimental validation

Computationally predicted top compounds were searched for their availability and ease of purchase. In total 10 compounds were ordered from Molport (https://www.molport.com). The details of compound number with their Molport ID are as follows: Compound 1(MolPort-001–740–483), Compound 2 (MolPort-021–804–591), Compound 3 (MolPort-001–740–229), Compound 4 (MolPort-001–741–384), Compound 5 (MolPort-005–945–341), Compound 6 (MolPort-002–515–588), Compound 7 (MolPort-000–779–136), Compound 8 (MolPort-002–132–868), Compound 9 (MolPort-001–740–491), Compound 10 (MolPort-046–509–064).

We also used VIPER and CP7 peptides as a positive and negative control, for cell-based reporter assay. These peptides were commercially available and were purchased from Novus Biologicals (https://www.novusbio.com/products/tlr4-inhibitor_nbp2–26244) [27]. We used VIPER peptide (KYSFKLILAEYRRRRRRRRR**)** as a known positive control [16,14] that is known to inhibit the downstream signaling thereby, lower the SEAP production. And along with it the CP7 peptide (RNTISGNIYSARRRRRRRRR) is a known negative control that does not affect the downstream signaling. These peptides are well established in the field and is commercially used as TLR4 inhibitor peptide set. The VIPER peptide for the NMR experiment was customized and ordered from Lifetime (https://www.lifetein.com/). The sequence from the VIPER motif used for the peptide was KYSFKLILAEY [27].

2.4. Cell-based SEAP reporter assay

HEK-Blue™ TLR4 cells (Invivo Gen- https://www.invivogen.com/hek-blue-htlr4) were used, to study the stimulation of TLR4 by monitoring the activation of NF-κB and AP-1. These cells have been also used for several similar studies for finding small molecule drug molecules [28–30].

These cells are already co-transfected by human TLR4, MD-2, and CD14 co-receptor genes, and an inducible SEAP reporter gene. The stable cell lines were grown in media containing DMEM, Fetal bovine serum (10 X FBS), Penicillin-Streptomycin-Glutamine (1 X PSG), and 1 X HEK-Blue™ Selection antibiotics. Cells were grown to 80 % confluency and then detached and counted. Cells were added to freshly prepared detection media with ~140,000 cells per ml. 180 μl of cell suspension solution (~25,000 cells) were added to each well of a 96-well plate. Further, we added the water/ peptide/ compounds (effective concentration of 100uM per well) and incubated it for one hour at 37 °C in 5 % CO2.

Lipopolysaccharide purified from Escherichia coli K12 (LPD-EK) was purchased from Invivogen (cat code: tlrl-peklps) for using as PAMP in TLR4 pathway activation [31]. This is an ultrapure form of LPS extracted by successive enzymatic hydrolysis step and purifies using phenol-TEA-DOC extraction protocol [32]. These do not contain lipoprotein, therby it only activated TLR4 pathway in the cells. LPS dose-dependent assay was performed initially to check for optimum LPS needed for TLR4 activation and SEAP production. Further, 10 ng/ml was found to be the optimum amount of LPS, and it was used as a ligand in screening compounds. For screening the compounds, we prepared a 100 mM stock of each compound in DMSO, and then prepared a working solution of 10 mM in water. We first used an effective concentration of 100 μM of each compound and checked for % LPS-induced SEAP production ((Absorbance LPS) / (Absorbance Control) * 100). This was further incubated for 24 h and then the SEAP produced was calculated. For this assay, we have also used positive (VIPER peptide), and negative controls (CP7 peptide) [27]. Compounds that performed better than positive control in the % LPS-induced SEAP production screening were further studied by performing the dose-dependent assay.

Here, HEK-Blue™ TLR4 cells were treated with various

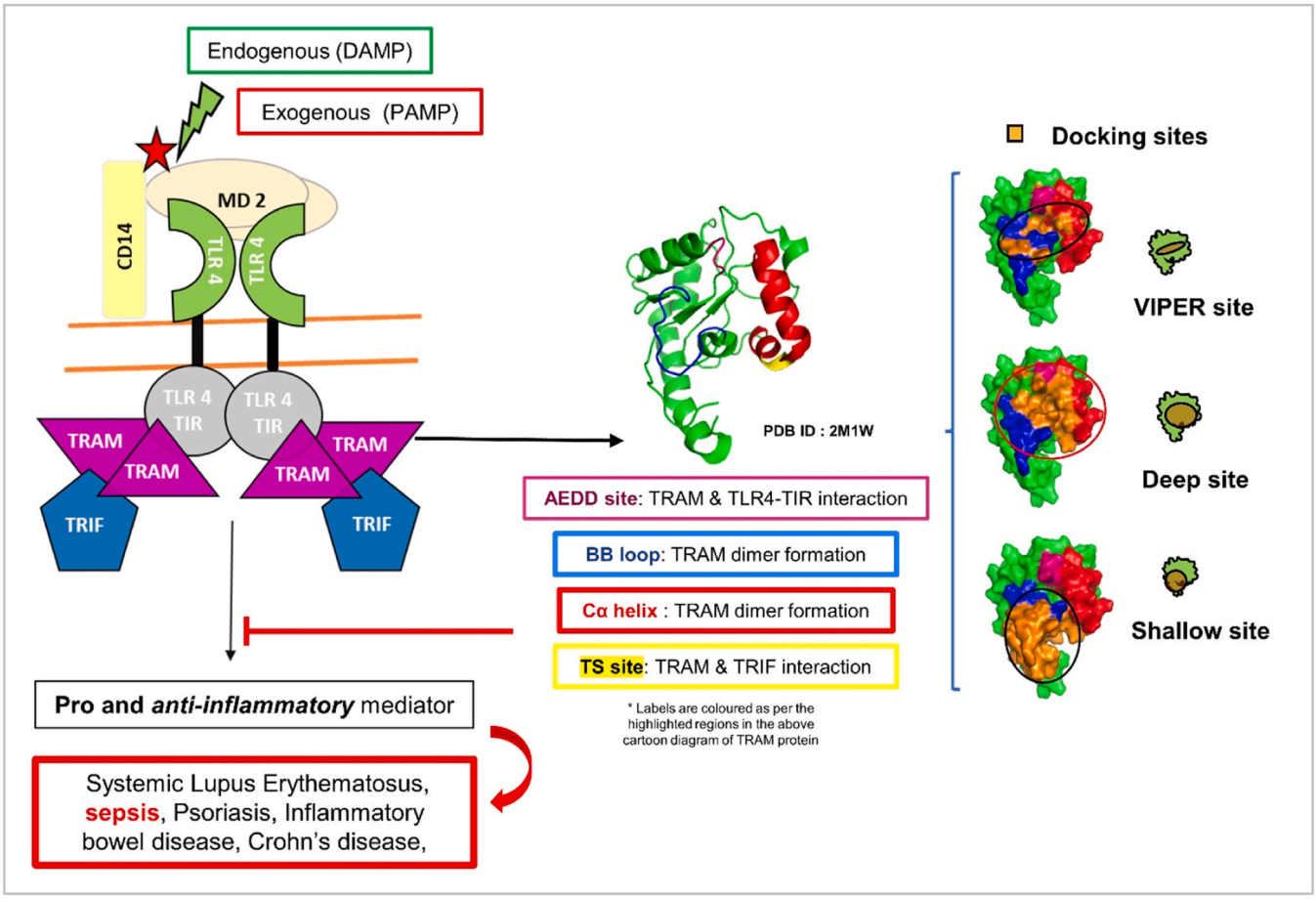

Fig. 2. A schematic of TRAM mediated TLR4 pathway leading to overproduction of inflammatory mediators in presence of excess PAMP and DAMPS causing autoimmune conditions. Highlighted residues on the TRAM cartoon structure depict AEDD site, BB loop, Cα helix, and TS site. The docking sites (VIPER, Deep, and Shallow) are shown on the surface cartoon diagram with important residues highlighted in different colors.

concentrations of compounds in serially diluted manner. Concentrations used were 100 μM, 50 μM, 25 μM, 12.5 μM, 6.25 μM, 3.125 μM, 1.5625 μM, 0.78125 μM. Dose-response curves were made for this concentration. The experiment was performed independently three times and % LPS induced SEAP production was calculated with respect to control. IC_{50} values (half maximal inhibitory concentration) were calculated for these by using Graphpad Prism 9 software (Y=Bottom + (TopBottom)/(1 +10ˆ((LogIC_{50}-X) *HillSlope)).

We also performed the MTT (3-(4,5-dimethylthiazol-2-yl)-2,5-diphenyltetrazolium bromide) tetrazolium reduction assay to check the viability of the cells. HEK-Blue™ TLR4 cells were initially seeded into 96 well plates, it was incubated for 48 h for cells to become adhesive and gain confluency for the experiment (40–60 %). After 48 h cells were treated with compounds in serially diluted concentrations (100 μM, 50 μM, 25 μM, 12.5 μM, 6.25 μM, 3.125 μM). Cells with treatment was incubated for another 24 h. Subsequently, MTT (0.5 mg/ml) solution was added to each well and incubated for 4 h. Next, incubation formazan crystal was dissolved using isopropanol and then absorbance was taken at 580 nm. The experiment was repeated in triplicates and cell viability was measured in presence of compounds.

2.5. Protein purification

The human TRAM gene (pcDNA3-TRAM-CFP, Plasmid #13027) was purchased from addgene (https://www.addgene.org/13027/#?). The region encoding the TIR domain (amino acid residues 70–235) was cloned into the pET28a (+) vector with restriction enzymes (*Nde*I and Hind lll) and expressed as a His6-tagged fusion protein at the N terminus. pET28a (+)-TRAM-TIR cloned vector was then transformed into Escherichia coli BL21(DE3). The transformed E. coli BL21(DE3) cells were cultured in N^{15} labeled ($N^{15}H_4Cl$) minimal media at 37 °C until the OD_{600} reached ~0.6–0.7. Composition of M9 Minimal media is shown in Supplementary Figure 11. The cells were induced with 1.0 mM IPTG and then cultured for 5 h at 37 °C. The harvested cells were resuspended in lysis buffer [50 mM Tris, 300 mM NaCl,1 mM PMSF, DNase 0.1 mg/ml, 5 mM MgCl2, pH 8.0] and lysed using sonication. TRAM-TIR fused with His6-tag was first purified by Ni2 + -NTA affinity chromatography (HisTrap H- 5 ml) with step elution of TRAM-TIR at 200 mM Imidazole concentration. The purified protein was concentrated and buffer exchange was done to 50 mM Tris, 150 mM NaCl, 1.5 mM CaCl2, pH 8.0. The concentrated protein was then treated with thrombin (SRP6556–1KU) for cleavage of His tag and after 4 h of cleavage at RT, 1 mM PMSF was added to stop the reaction and finally, size exclusion chromatography (Superdex 75 16/600) was done in 50 mM HEPES, 5 mM DTT, 0.1 mM EDTA, pH= 7.4. The labeled protein was then used for conducting NMR titration experiments. The protein purification profile with steps of Affinity and size exclusion chromatography is shown in Supplementary Figure 12.

2.6. NMR titration experiment

The compounds were diluted to a concentration of 5 mM in protein buffer and titrated with protein in the following ratios (1:0, 1:1, 1:2, 1:4). HSQC data were collected for all the runs for compounds 2, 3, 4, 9, 10 and VIPER peptide.

Chemical shift perturbations were calculated using the formula: CSP

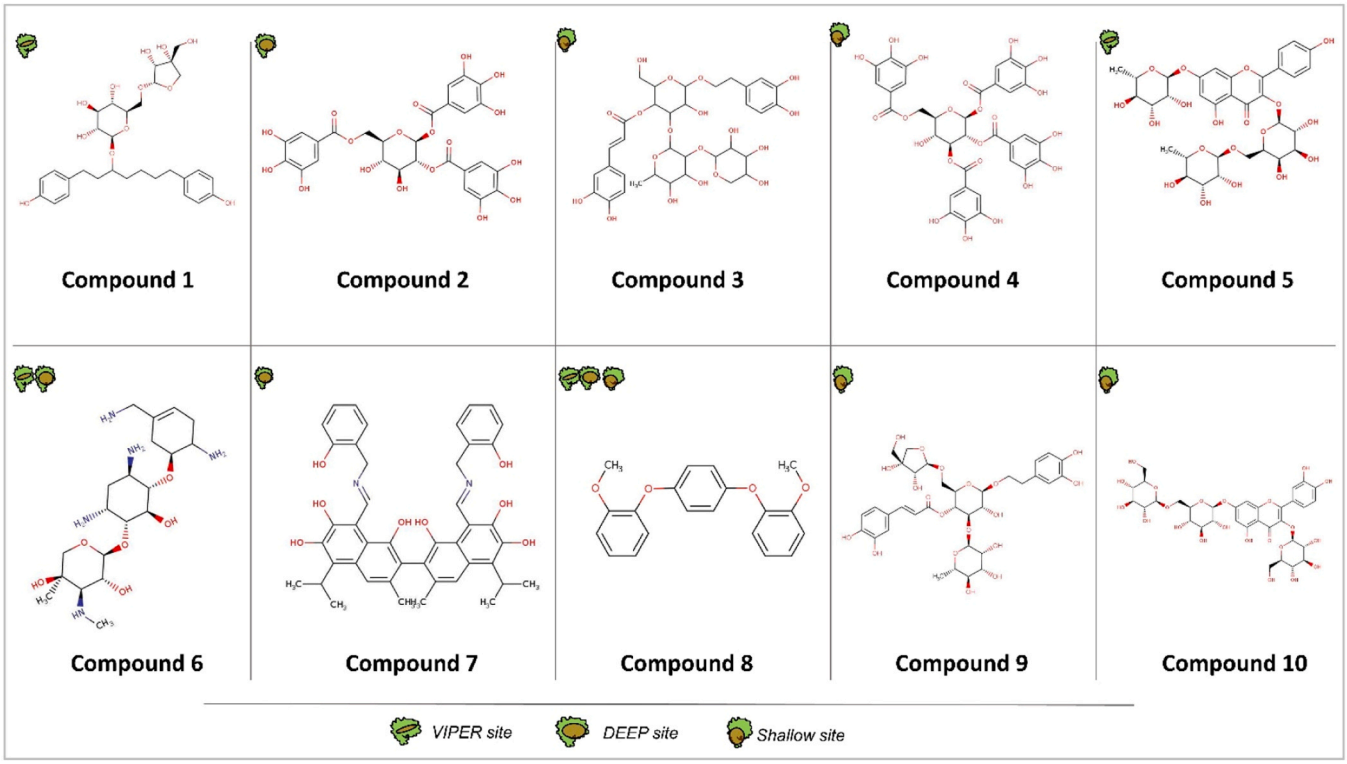

Fig. 3. Chemical structure of top ten ligands selected from Virtual screening along with their binding sites.

$= [(\Delta\delta HN)^2 + (\Delta\delta N)^2/25]^{1/2}$ [33]. All NMR spectra were acquired at 25 °C on 800 MHz/600 MHz Bruker Avance III spectrometers, processed using NMRPipe, and analyzed using Spar [34,35].

3. Results and discussions

3.1. Putative binding sites on the TRAM protein

Potential binding sites on TRAM were chosen such that it interferes with the binding of TRAM to TLR4-TIR or TRIF and thereby abrogating the downstream signaling. The residues of TRAM that were part of binding pockets for the VIPER peptide were selected as one of the putative binding sites – we refer this as "VIPER site" (Fig. 2). We also used SITEMAP within Schrodinger package to predict other potential binding sites. Two other sites were selected using SITEMAP which are named "Deep" and "Shallow" sites (as marked in Fig. 2) on the basis of ligand binding score, docking score, size and volume of the pocket (listed in Supplementary Figure 1).

These pockets also contain structurally important residues like AEDD and TS site, that are involved in upstream TLR4-TIR and downstream TRIF interaction with TRAM respectively. Along with these sites, residues from the BB loop and Cα helix that are important for dimer formation are also included in the docking sites.

3.2. Virtual screening against TLR4 adaptor molecule TRAM-TIR

Virtual screening was performed at pH = 7.4 using the three docking pockets of TRAM protein against the Supernatural II database that consists of 3,25,287 ligands [18]. With a rigorous screening of the naturally derived small molecule library using steps of virtual screening (HTVS, SP, and XP) we filtered the dataset to a smaller number, around 3500 small molecules. Further with the energy scores, and ADMET properties, we clustered top hits using various clustering approaches to get the best representative of the small molecules. Finally, the top ten hits were selected and extensively searched in literature for their known properties. The curated list of the top ten compounds is provided in Fig. 3. Other details like SMILES format, docking scores, binding energy values, and availability of these compounds are mentioned in Supplementary Figure 2.

Most of the small molecules are associated with anti-inflammatory, antipyretic and antioxidant properties. Some are of Asian origin and have been documented as regularly used in traditional Chinese medicines. In particular, Compound 1 is found in plants like *Betula platyphylla* (common name: Asian white birch) and *Acer maximowiczinum* (common name: Nikko maple, native to China and Japan). It is an HDAC6 inhibitor that synergistically enhances anticancer activity [36]. Compound 2 obtained from the cell culture of *Cornus Officinalis* (common name: Japanese cornel dogwood) which has antiviral properties and works as an inhibitor of HCV NS3 Protease and Vertebrate Squalene Epoxide [37]. Compound 3 is found in the stem bark of *Magnolia officinalis* (common name: Chinese Magnolia) has antioxidant properties and is used in traditional Chinese medicines [38]. Compound 4 is found in fruits like *Punica granatum* (pomegranate) and *Mangifera indica* (mango). It shows anti-microbial, anti-inflammatory, antioxidant, and anti-carcinogenic properties [39]. Compound 5 found in *Vinca erecta* (European periwinkle) and Robinia pseudoacaia (White Locust Tree) mentioned in traditional Chinese medicine has anti-bacterial, anti-inflammatory, and diuretic properties [40]. Compound 6 has a scaffold that was an integral part of many other top hits natural compounds. Compounds 7 and 8, albeit recognised from the Supernatural II database, do not have evidence of their use in literature. Compound 9 is found in leaves of *Lamioplomis rotate (Benth.) Kudo* (known as Dabuba in Tibet and China) and is used as a Chinese folk medicine plant for an anti-inflammatory condition like sepsis [41]. It is known to inhibit TNF-alpha, IL-6, and IκB and modulate NF-κb. Compound 10 is found in the seed of *Desuranina Sophia* (flixweed or tansy mustard) and has anti-inflammatory, antipyretic, analgesic, antioxidant, and anthelmintic properties [42].

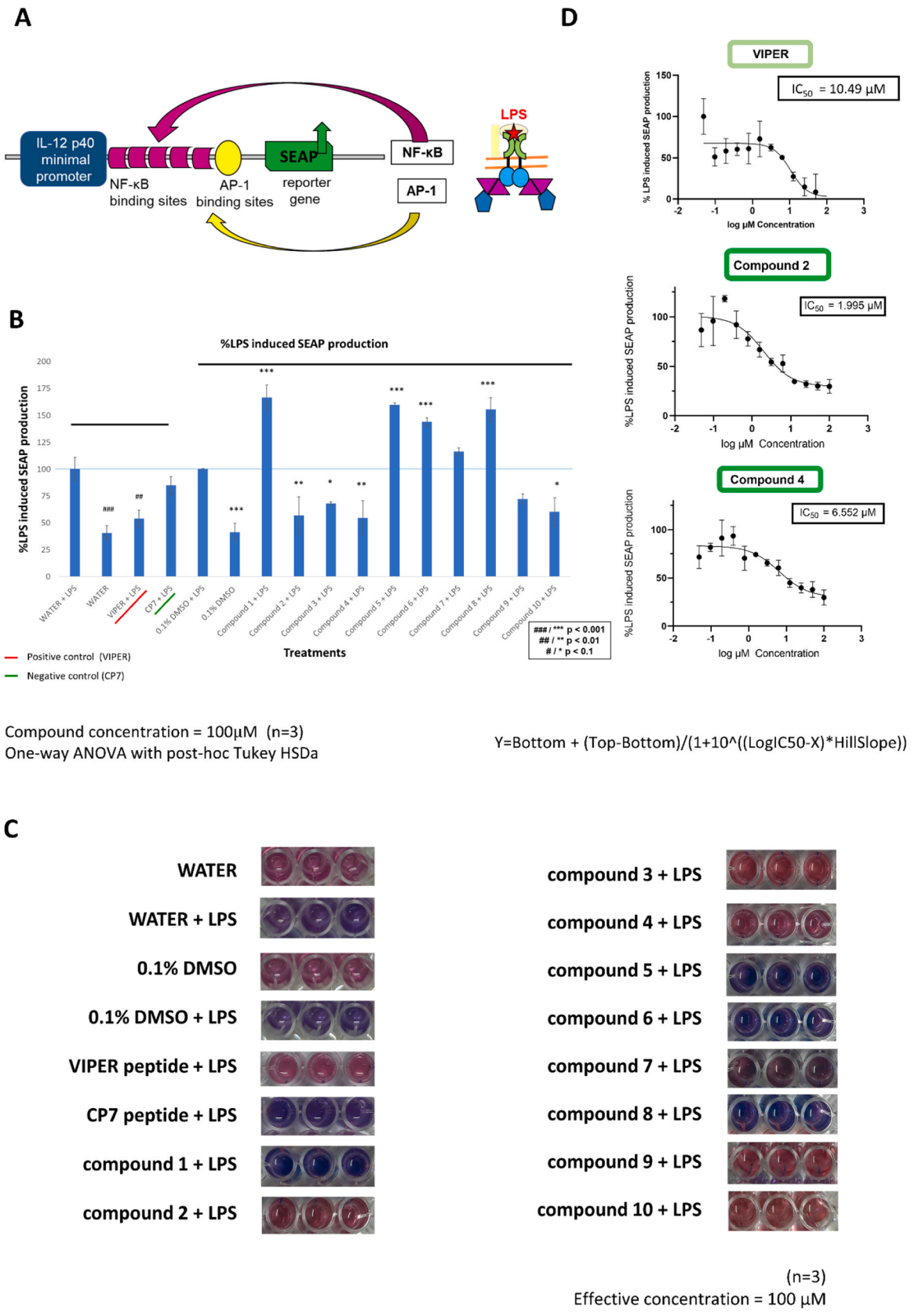

Fig. 4. A) Schematic depicting the activation of TLR4 complex in presence of LPS and thereby producing NF-kB and AP-1. These transcription factor bind to their respective binding sites downstream of the SEAP reporter gene. These lead to SEAP production by the HEK Blue TLR4 cells. B) Graph shows the % LPS induced SEAP production in presence of compounds at 100 µM concentration. C) Observed colour change while screening of compounds using cell-based reporter assay to validate the SEAP production. D) Dose-dependent assay for VIPER peptide, Compounds 2, and 4 to calculate the IC_{50} values.

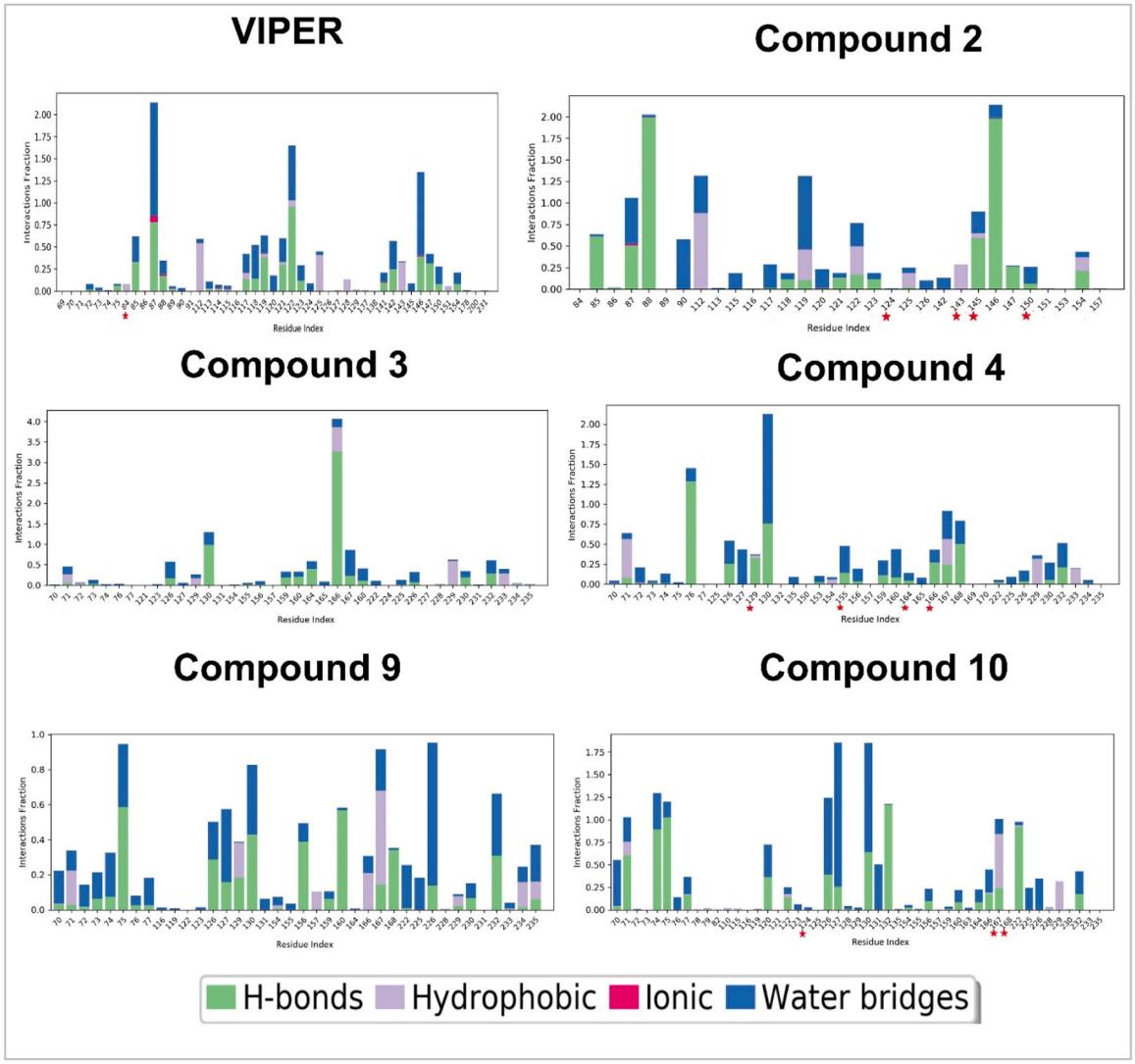

Fig. 5. Stacked bar blot showing residues involved in H-bonds, Hydrophobic, Ionic, and Water bridges. The results are plotted as per the 100 ns MD simulation trajectories for VIPER peptide, Compounds 2, 3, 4, 9, and 10 docked complexes. Residues highlighted with a red star are also found significantly interacting in the NMR titration experiment (**VIPER**: LEU_84, **Compound 2**: ASN_124, PHE_143, ARG_145, ASN_150, **Compound 4**: VAL_129, THR_155, GLN_164, LYS_166, **Compound 10**: ASN_124, TYR_167, ASN_168).

3.3. Reporter gene assay using HEK-Blue hTLR4 cells

We screened the top compounds using cell-based reporter assay and found Compounds 2, 3, 4, 9, and 10 were inhibiting TLR4 activation in presence of ligand (LPS). The inhibition by these compounds were comparable to the known positive control i.e. VIPER peptide. The LPS optimization values and SEAP assay for compounds are shown in Supplementary Figure 3. We also performed dose-dependent assay to calculate the IC_{50} value of the compounds and found Compounds 2 and 4 inhibits the activity at IC_{50} of 1.995 μM and 6.552 μM respectively. Based on the IC_{50}, both the compounds have higher efficacy against TLR4 signaling as compared to know inhibition by VIPER peptide (IC_{50} of 10.49 μM). Results from dose dependent assay of other compounds are shown in Supplementary Figure 3. A figure depicting the schematic of the functioning of HEK-Blue hTLR4 cells, LPS-induced cell-based reporter screening assay, and dose-dependent assay for compounds (VIPER, Compound 2 and 4) that are inhibiting the downstream signaling is shown in Fig. 4 and for Compound 3, 9 and 10 is shown in Supplementary Figure 4. We also performed cell viability assay to check the toxicity of these compounds. This cell viability assay was done in the absence of LPS and using range of concentration of small molecule compound (100 μM, 50 μM, 25 μM, 12.5 μM, 6.25 μM, 3.125 μM). As these are small molecule compounds of natural origin, they are expected and found to cause no toxicity to cells. The results are shown in Supplementary Figure 5.

Additionally, compounds 1, 5, 6, and 8 were increasing the SEAP production. It may be binding to TRAM in such a way that strengthen the downstream signaling. Thereby, these may act as potential agonists for the TRAM-mediated TLR4 signaling pathway.

3.4. Molecular dynamics simulations for best ligand-protein complexes

The strength of small molecule ligand interaction with TRAM protein was verified using MD simulations. We observed the Root Mean Square Deviation (RMSD) of protein and ligand from the reference frame to measure the changes in the position of atoms. Protein appears to be stable by the end of the simulation in each case. We also looked at Root Mean Square Fluctuations of the protein to determine the protein region involved in major interactions and see if the secondary structures were maintained across the trajectory. The trend of these values across trajectory for TRAM protein is in Supplementary Figure 6, 7 and 8 respectively.

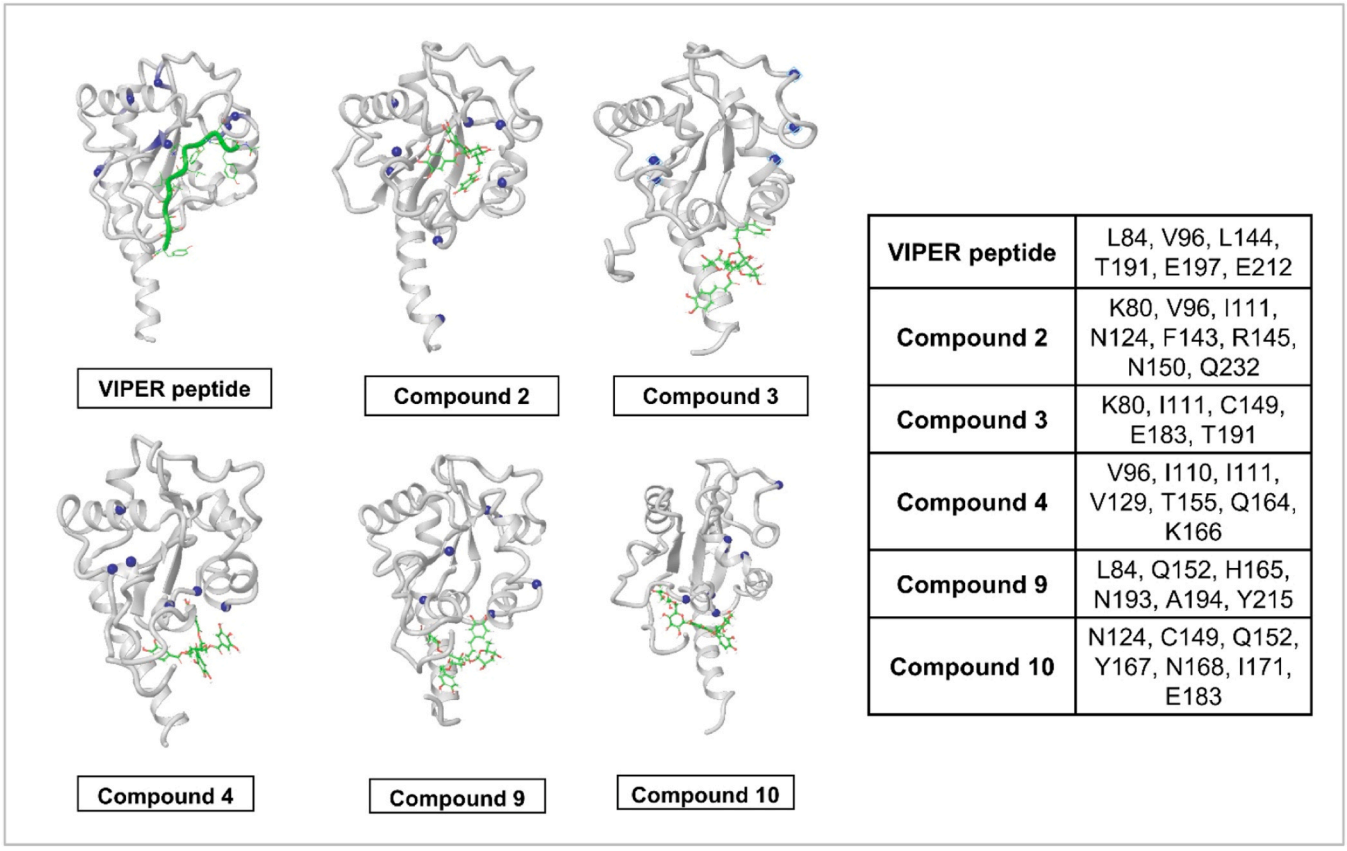

VIPER peptide	L84, V96, L144, T191, E197, E212
Compound 2	K80, V96, I111, N124, F143, R145, N150, Q232
Compound 3	K80, I111, C149, E183, T191
Compound 4	V96, I110, I111, V129, T155, Q164, K166
Compound 9	L84, Q152, H165, N193, A194, Y215
Compound 10	N124, C149, Q152, Y167, N168, I171, E183

Fig. 6. Cartoon diagram of TRAM protein in docked pose from final frame of molecular dynamics run (100th ns frame). Residues highlighted in blue show CSP higher than average CSP + 2 SD. The table on the right lists the position and name of the residues identified as significantly interacting with each of the compounds through NMR titration experiments.

Apart from these, we also monitored the protein-ligand contacts throughout the simulation. These interactions were categorized mainly into four major categories: Hydrogen Bonds, Hydrophobic, Ionic, and Water Bridges. Interactions that were consistent for 70 % of the simulation are shown in the stacked bar plot in Fig. 5. A schematic for the simulation interaction diagram for ligands docked pose in protein pocket is shown in Supplementary Figure 9.

3.5. NMR protein-ligand titration studies

Some of the residues identified through the simulation interaction diagram are significantly found to be interacting in the NMR titration experiment as shown in Fig. 5. While performing the NMR titration with each protein-ligand complex, the residues which show Chemical shift perturbations (CSP) more than the average value + 2 SD (standard deviation) are highlighted in the images below. For the pictorial representation final frame snapshots (100th ns) from each protein-ligand complex were taken and interacting residues as observed in NMR are highlighted in blue color (CSP > average CSP + 2 SD) (Fig. 6). A detailed plot with CSP values for each complex is shown in Supplementary Figure 10.

Through both the computational and experimental NMR studies, following list of residues were found to be consistent at the interaction site of small molecule compounds and TRAM. Residues N124, F143, R145, N150 for Compound 2; V129, T155, Q164, K166 for Compound 4, and N124, Y167, N168 for Compound 10. Among these residues, N124 and V129 are part of the second alpha helix that is structurally after the BB loop region. Residues F143, R145, and N150 are part of the third alpha helix (Cα helix) that is important for TRAM dimer interface. Residue T155 is part of the fourth alpha helix and it forms the TS site that is important for the interaction of TRAM-TIR with TRIF for downstream signaling. Apart from these, other residues i.e., Q164, K166, Y167, and N168 are part of the loop region connecting the fourth and fifth helix. Amongst these, Y167 is a crucial residue since its mutation leads to complete loss of phosphorylation in response to LPS [43]. Interestingly, in the case of Compounds 3 and 4, we noticed several residues that are far from the predicted binding site. This may imply presence of allosteric binding site or some structural changes occurring at distant residue because of ligand binding. This can be because of long distance interaction occurring in protein structures. A network-based approach can highlight these better, which is currently out of the scope of the paper. Some literature which supports such long range allostery due to ligand binding has been cited [44,45].

4. Conclusion

Overall, the study aims to target the TLR4 pathway in case of overproduction of pro and anti-inflammatory mediators leading to autoimmune conditions. We selected the TRAM adaptor protein as the potential candidate for our study to target TRAM mediated TLR4 pathway. We screened the docking sites against ligands from natural origin followed by extensive steps of filtering, binding energy scoring, clustering, and selecting the top hits. We also extended our computational study to perform the cell-based assay for validating the effect of compounds in HEK-Blue™ TLR4 cells. We performed dose-dependent assay and calculated the IC_{50} value. Further, we purified the TRAM-TIR domain and performed NMR titration experiments to verify the interacting residues in vitro. The involvement of these residues in the significant interaction of small molecules and TRAM protein can interfere with the signaling of TRAM with its downstream TRIF and while forming dimers.

The current approach targets the structurally important regions like the BB loop, Cα helix, TS site, and phosphorylation site.

Altogether using our integrated approach, we identified Compound 2 and Compound 4 as promising hits and probable antagonists for TRAM protein. Compound 2 binds 10 times better than the control VIPER peptide as measured by the reporter assay, whereas Compound 4 retains 60 % lower IC_{50} value in comparison with this peptide. These two compounds also affect the structural positions of multiple residues through NMR titrations. Much of these interactions, especially hydrogen bonds, are retained throughout the MD simulations. These naturally derived small molecule compounds can be useful for abrogating the downstream signaling in case of autoimmune disorders.

A potential limitation of the study will be false negatives, due to our stringent filtering. In addition, the initial docking considers target protein structure as a rigid entity, although multiple docking poses were taken into consideration for selecting the best possible pose. We also used the clustering method to choose the best representative of similar structures. The cluster centroids were, therefore, considered as top hits. Further, cluster members were next selected as secondary hits and the experiments were performed. However, none of the secondary hits were observed to bind better than the initial set of hits (data not shown).

Apart from this, the experiments were conducted using HEK-Blue™ TLR4 cells, replicating the same on other cell lines will give more insight into the behavior and efficacy of these compounds. But as the major objective was to validate these compounds, our LPS dose-dependent assay provides confidence for computationally predicted compounds. Further, the top hits can be used as parent structure and chemically modified to promote stronger binding and be developed as a stronger antagonist against TRAM-mediated TLR4 signaling pathway.

Ethics approval and consent to participate

Not applicable.

Credit authorship contribution statement

SV carried out all the experiments and analyses. SV and PR carried out NMR analyses. RS and SV conceptualized the study. SV wrote the first draft of the manuscript. All authors improved the manuscript.

Declaration of Competing Interest

The authors declare that the research was conducted in the absence of any commercial or financial relationships that could be construed as a potential conflict of interest.

Acknowledgements

The authors would like to thank NCBS (TIFR) for infrastructural facilities. They would like to thank Dr Vinoth Kumar, Dr Praveen Vemula and Dr Ranabir Das for useful discussions. The authors would also thank Shaileshanand Jha, Tripti Kharbanda, Radhika Rao and Rajamohammed Khader for helping with experiments. RS acknowledges funding and support provided by JC Bose Fellowship (JBR/2021/000006) from Science and Engineering Research Board, India and Bioinformatics Centre Grant funded by Department of Biotechnology, India (BT/PR40187/BTIS/137/9/2021). RS would also like to thank Institute of Bioinformatics and Applied Biotechnology for the funding through her Mazumdar-Shaw Chair in Computational Biology (IBAB/MSCB/182/2022).

Appendix A. Supporting information

Supplementary data associated with this article can be found in the online version at doi:10.1016/j.csbj.2023.07.026.

References

[1] Vidya MK, Kumar VG, Sejian V, Bagath M, Krishnan G, Bhatta R. Toll-like receptors: significance, ligands, signaling pathways, and functions in mammals. Int Rev Immunol 2018. https://doi.org/10.1080/08830185.2017.1380200.
[2] Botos I, Segal DM, Davies DR. The structural biology of toll-like receptors. Structure 2011. https://doi.org/10.1016/j.str.2011.02.004.
[3] Slack JL, et al. Identification of two major sites in the type I interleukin-1 receptor cytoplasmic region responsible for coupling to pro-inflammatory signaling pathways. J Biol Chem 2000. https://doi.org/10.1074/jbc.275.7.4670.
[4] Essuman K, et al. TIR domain proteins are an ancient family of NAD+-consuming enzymes. e4 Curr Biol 2018;28(3):421–30. https://doi.org/10.1016/j.cub.2017.12.024.
[5] Loring HS, et al. A phase transition enhances the catalytic activity of sarm1, an nad + glycohydrolase involved in neurodegeneration. Elife 2021;10:1–33. https://doi.org/10.7554/eLife.66694.
[6] Zughaier SM, Zimmer SM, Datta A, Carlson RW, Stephens DS. Differential induction of the toll-like receptor 4-MyD88-dependent and -independent signaling pathways by endotoxins. Infect Immun 2005;73(5):2940–50. https://doi.org/10.1128/IAI.73.5.2940-2950.2005.
[7] Tan Y, Zanoni I, Cullen TW, Goodman AL, Kagan JC. Mechanisms of toll-like receptor 4 endocytosis reveal a common immune-evasion strategy used by pathogenic and commensal bacteria. Immunity 2015. https://doi.org/10.1016/j.immuni.2015.10.008.
[8] Miguel RN, et al. A dimer of the toll-like receptor 4 cytoplasmic domain provides a specific scaffold for the recruitment of signalling adaptor proteins. PLoS One 2007. https://doi.org/10.1371/journal.pone.0000788.
[9] Y. Enokizono et al., Structures and interface mapping of the TIR domaincontaining adaptor molecules involved in interferon signaling, Proc Natl Acad Sci. U S A, 2013, doi: 10.1073/pnas.1222811110.
[10] Anwar MA, Shah M, Kim J, Choi S. Recent clinical trends in Toll-like receptor targeting therapeutics. Med Res Rev 2019. https://doi.org/10.1002/med.21553.
[11] Martin GS. Sepsis, severe sepsis and septic shock: changes in incidence, pathogens and outcomes. Expert Rev Anti Infect Ther 2012;10(6):701–6. https://doi.org/10.1586/eri.12.50.
[12] Torrecillas FCalbo. Germs. Esp Pedia 1989;31(Suppl 3):165–72. https://doi.org/10.1177/000992288702600906.
[13] Savva A, Roger T. Targeting Toll-like receptors: promising therapeutic strategies for the management of sepsis-associated pathology and infectious diseases. Front Immunol 2013;4(NOV):1–16. https://doi.org/10.3389/fimmu.2013.00387.
[14] Mahita J, Harini K, Pichika MR, Sowdhaminia R. An in silico approach towards the identification of novel inhibitors of the TLR-4 signaling pathway. J Biomol Struct Dyn 2015. https://doi.org/10.1080/07391102.2015.1079243.
[15] Lysakova-Devine T, et al. Viral inhibitory peptide of TLR4, a peptide derived from vaccinia protein A46, specifically inhibits TLR4 by directly targeting MyD88 adaptor-like and TRIF-related adaptor molecule. J Immunol 2010;185(7):4261–71. https://doi.org/10.4049/jimmunol.1002013.
[16] Stack J, Bowie AG. Poxviral protein A46 antagonizes toll-like receptor 4 signaling by targeting BB loop motifs in Toll-IL-1 receptor adaptor proteins to disrupt receptor: adaptor interactions. J Biol Chem 2012;vol. 287(27):22672–82. https://doi.org/10.1074/jbc.M112.349225.
[17] ichiro Oda S, Franklin E, Khan AR. Poxvirus A46 protein binds to TIR domain-containing Mal/TIRAP via an α-helical sub-domain. Mol Immunol 2011;48(15–16):2144–50. https://doi.org/10.1016/j.molimm.2011.07.014.
[18] Banerjee P, Erehman J, Gohlke BO, Wilhelm T, Preissner R, Dunkel M. Super natural II-a database of natural products. Nucleic Acids Res 2015. https://doi.org/10.1093/nar/gku886.
[19] Friesner RA, et al. Extra precision glide: docking and scoring incorporating a model of hydrophobic enclosure for protein-ligand complexes. J Med Chem 2006. https://doi.org/10.1021/jm051256o.
[20] Halgren TA. Identifying and characterizing binding sites and assessing druggability. J Chem Inf Model 2009. https://doi.org/10.1021/ci800324m.
[21] W.L. Jorgensen, QikProp, Schrödinger LLC, New York. 2016.
[22] Genheden S, Ryde U. The MM/PBSA and MM/GBSA methods to estimate ligand-binding affinities. Expert Opin Drug Discov 2015. https://doi.org/10.1517/17460441.2015.1032936.
[23] Duan J, Dixon SL, Lowrie JF, Sherman W. Analysis and comparison of 2D fingerprints: Insights into database screening performance using eight fingerprint methods. J Mol Graph Model 2010. https://doi.org/10.1016/j.jmgm.2010.05.008.
[24] Sastry M, Lowrie JF, Dixon SL, Sherman W. Large-scale systematic analysis of 2D fingerprint methods and parameters to improve virtual screening enrichments. J Chem Inf Model 2010. https://doi.org/10.1021/ci100062n.
[25] Schrödinger Release, Desmond molecular dynamics system Schrödinger LLC, 2019.
[26] Jorgensen WL, Chandrasekhar J, Madura JD, Impey RW, Klein ML. Comparison of simple potential functions for simulating liquid water. J Chem Phys 1983;79(2):926–35. https://doi.org/10.1063/1.445869.
[27] Kim Y, Lee H, Heo L, Seok C, Choe J. Structure of vaccinia virus A46, an inhibitor of TLR4 signaling pathway shows the conformation of VIPER motif. Protein Sci 2014;23(7):906–14. https://doi.org/10.1002/pro.2472.
[28] Hu Z, et al. Small-Molecule TLR8 antagonists via structure-based rational design. e3 Cell Chem Biol 2018;25(10):1286–91. https://doi.org/10.1016/j.chembiol.2018.07.004.
[29] Salyer ACD, Caruso G, Khetani KK, Fox LM, Malladi SS, David SA. Identification of adjuvantic activity of amphotericin B in a novel, multiplexed, poly-TLR/NLR high-throughput screen. PLoS One 2016;11(2):1–17. https://doi.org/10.1371/journal.pone.0149848.

[30] Pérez-Regidor L, et al. Small molecules as toll-like receptor 4 modulators drug and in-house computational repurposing. Biomedicines 2022;10(9). https://doi.org/10.3390/biomedicines10092326.
[31] Kuhnert P, Nicolet J, Frey J. Rapid and accurate identification of Escherichia coli K-12 strains. Appl Environ Microbiol 1995;61(11):4135–9. https://doi.org/10.1128/aem.61.11.4135-4139.1995.
[32] Hirschfeld M, Ma Y, Weis JH, Vogel SN, Weis JJ. Cutting edge: repurification of lipopolysaccharide eliminates signaling through both human and murine toll-like receptor 2. J Immunol 2000;165(2):618–22. https://doi.org/10.4049/jimmunol.165.2.618.
[33] Grzesiek S, Stahl SJ, Wingfield PT, Bax A. The CD4 determinant for downregulation by HIV-1 Nef directly binds to Nef. Mapping of the Nef binding surface by NMR. Biochemistry 1996;35(32):10256–61. https://doi.org/10.1021/bi9611164.
[34] Delaglio F, Grzesiek S, Vuister GW, Zhu G, Pfeifer J, Bax A. NMRPipe: a multidimensional spectral processing system based on UNIX pipes. J Biomol NMR 1995;6(3):277–93. https://doi.org/10.1007/BF00197809.
[35] Lee W, Tonelli M, Markley JL. NMRFAM-SPARKY: enhanced software for biomolecular NMR spectroscopy. Bioinformatics 2015;31(8):1325–7. https://doi.org/10.1093/bioinformatics/btu830.
[36] Ryu HW, Lee DH, Shin DH, Hyun Kim S, Kwon SH. Aceroside VIII is a new natural selective hdac6 inhibitor that synergistically enhances the anticancer activity of HDAC inhibitor in HT29 cells. Planta Med 2015. https://doi.org/10.1055/s-0034-1396149.
[37] Duan D, Li Z, Luo H, Zhang W, Chen L, Xu X. Antiviral compounds from traditional Chinese medicines Galla Chinese as inhibitors of HCV NS3 protease. Bioorg Med Chem Lett 2004. https://doi.org/10.1016/j.bmcl.2004.09.067.
[38] Yu SX, Yan RY, Liang RX, Wang W, Yang B. Bioactive polar compounds from stem bark of Magnolia officinalis. Fitoterapia 2012. https://doi.org/10.1016/j.fitote.2011.11.020.
[39] Torres-León C, Ventura-Sobrevilla J, Serna-Cock L, Ascacio-Valdés JA, Contreras-Esquivel J, Aguilar CN. Pentagalloylglucose (PGG): a valuable phenolic compound with functional properties. J Funct Foods 2017. https://doi.org/10.1016/j.jff.2017.07.045.
[40] J. Zhou, G. Xie, and X. Yan, Encyclopedia of Traditional Chinese Medicines - molecular structures, pharmacological activities, natural sources and applications. 2011.
[41] Jiang WL, Yong-Xu SP, Zhang HB, Zhu, Jian-Hou. Forsythoside B protects against experimental sepsis by modulating inflammatory factors. Phytother Res 2012. https://doi.org/10.1002/ptr.3668.
[42] Nimrouzi M, Zarshenas MM. Phytochemical and pharmacological aspects of Descurainia sophia Webb ex Prantl: modern and traditional applications. Avicenna J Phytomed 2016;6(3):266–72. https://doi.org/10.22038/ajp.2016.4469.
[43] Huai W, et al. Phosphatase PTPN4 preferentially inhibits TRIF-dependent TLR4 pathway by dephosphorylating TRAM. J Immunol 2015. https://doi.org/10.4049/jimmunol.1402183.
[44] Strotz D, et al. Protein allostery at atomic resolution. Angew Chem - Int Ed 2020;59(49):22132–9. https://doi.org/10.1002/anie.202008734.
[45] Ragona L, et al. NMR dynamic studies suggest that allosteric activation regulates ligand binding in chicken liver bile acid-binding protein. J Biol Chem 2006;281(14):9697–709. https://doi.org/10.1074/jbc.M513003200.